FHWA/IN/JTRP-2005/13

Final Report

STATEWIDE WIRELESS COMMUNICATIONS PROJECT

Volume 2: Inductive Loop Detection of Bicycles and Inductive Loop Signature Processing for Travel Time Estimation

James V. Krogmeier
Darcy M. Bullock

July 2008

Final Report

FHWA/IN/JTRP-2005/13

STATEWIDE WIRELESS COMMUNICATIONS PROJECT

Volume 2: Inductive Loop Detection of Bicycles and Inductive Loop Signature Processing for Travel Time Estimation

By

James V. Krogmeier
Associate Professor
School of Electrical and Computer Engineering
Purdue University

and

Darcy M. Bullock
Professor
School of Civil Engineering
Purdue University

Joint Transportation Research Program
Project No. C-36-75O
File No. 8-9-15
SPR-2852

Conducted in Cooperation with the
Indiana Department of Transportation
and the U.S. Department of Transportation
Federal Highway Administration

Purdue University
West Lafayette, IN 47907
July 2008

TECHNICAL REPORT STANDARD TITLE PAGE

1. Report No.	2. Government Accession No.	3. Recipient's Catalog No.
FHWA/IN/JTRP-2005/13		

4. Title and Subtitle	5. Report Date
Statewide Wireless Communications Project	July 2008
	6. Performing Organization Code

7. Author(s)	8. Performing Organization Report No.
J. V. Krogmeier and D. M. Bullock	FHWA/IN/JTRP-2005/13

9. Performing Organization Name and Address	10. Work Unit No.
Joint Transportation Research Program 1284 Civil Engineering Building Purdue University West Lafayette, IN 47907-1284	
	11. Contract or Grant No. SPR-2852

12. Sponsoring Agency Name and Address	13. Type of Report and Period Covered
Indiana Department of Transportation State Office Building 100 North Senate Avenue Indianapolis, IN 46204	Final Report
	14. Sponsoring Agency Code

15. Supplementary Notes

Prepared in cooperation with the Indiana Department of Transportation and Federal Highway Administration.

16. Abstract

The Statewide Wireless Communications Project was an umbrella project intended to support various INDOT activities in the area of wireless communications. As these activities were conducted independently the report for the project is organized into three volumes. Volume 1 contains the results of satellite and cellular communications field testing undertaken in support of INDOT's SiteManager application. Volume 1 also contains the results of an evaluation of spread spectrum radios for long-range communications. Volume 2 contains the results of detection zone evaluation for loop detection of bicycles and the results of testing algorithms for travel time estimation using vehicle re-identification based on inductive and micro-loop signatures. Finally, Volume 3 contains the results of preliminary testing of a vehicle-infrastructure integration application in road condition monitoring. In Volume 1 we found that SiteManager could not be adequately run over a satellite link because the long round trip delay of the communication link negatively interacted with SiteManager's internal client-server communications protocol to severely reduce overall throughput. A solution to the problem was to use terminal emulation in the field with the client software running on a computer connected to the server via a high bandwidth, low delay link. The downside to the terminal emulation approach is that it requires that the field engineer have a communication link wherever the application is run. In Volume 1 we also found that current generation spread spectrum radio ranges in Indiana topography with antenna heights corresponding to signal arm mounting were on the order of 3 miles. This was too short by a factor of 3 to support a multihop network for traffic signal control and telemetry. In Volume 2 we developed a numerical technique for mapping the bicycle detection zones of loop detectors. A number of recommendations were made concerning loop geometry, depth, detector sensitivity, and pavement markings for purposes of improving bicycle detection. We also developed algorithms for travel time estimation based on vehicle signatures captured from commercially available inductive and micro-loop detector cards. The travel time estimation algorithms were field tested and show promise. In Volume 3 a prototype road condition monitoring system was built upon a passenger van platform and preliminary field testing and data analysis was done. Algorithms were developed to address positional uncertainties present in GPS measurements in order to allow the averaging of data taken in multiple independent runs. The results were also field tested using INDOT's Laser Profiling vehicle.

17. Key Words	18. Distribution Statement
satellite communications, TCP/IP, spread spectrum radios, inductive and micro-loop detection, vehicle-infrastructure integration.	No restrictions. This document is available to the public through the National Technical Information Service, Springfield, VA 22161

19. Security Classif. (of this report)	20. Security Classif. (of this page)	21. No. of Pages	22. Price
Unclassified	Unclassified	Vol 1 – 42 Vol 2 – 37 Vol 3 - 31	

Form DOT F 1700.7 (8-69)

Abstract:

The Statewide Wireless Communications Project was an umbrella project intended to support various INDOT activities in the area of wireless communications. As these activities were conducted independently the report for the project is organized into three volumes. Volume 1 contains the results of satellite and cellular communications field testing undertaken in support of INDOT's SiteManager application. Volume 1 also contains the results of an evaluation of spread spectrum radios for long-range communications. Volume 2 contains the results of detection zone evaluation for loop detection of bicycles and the results of testing algorithms for travel time estimation using vehicle re-identification based on inductive and micro-loop signatures. Finally, Volume 3 contains the results of preliminary testing of a vehicle-infrastructure integration application in road condition monitoring.

In Volume 1 we found that SiteManager could not be adequately run over a satellite link because the long round trip delay of the communication link negatively interacted with SiteManager's internal client-server communications protocol to severely reduce overall throughput. A solution to the problem was to use terminal emulation in the field with the client software running on a computer connected to the server via a high bandwidth, low delay link. The downside to the terminal emulation approach is that it requires that the field engineer have a communication link wherever the application is run. In Volume 1 we also found that current generation spread spectrum radio ranges in Indiana topography with antenna heights corresponding to signal arm mounting were on the order of 3 miles. This was too short by a factor of 3 to support a multihop network for traffic signal control and telemetry.

In Volume 2 we developed a numerical technique for mapping the bicycle detection zones of loop detectors. A number of recommendations were made concerning loop geometry, depth, detector sensitivity, and pavement markings for purposes of improving bicycle detection. We also developed algorithms for travel time estimation based on vehicle signatures captured from commercially available inductive and micro-loop detector cards. The travel time estimation algorithms were field tested and show promise.

In Volume 3 a prototype road condition monitoring system was built upon a passenger van platform and preliminary field testing and data analysis was done. Algorithms were developed to address positional uncertainties present in GPS measurements in order to allow the averaging of data taken in multiple independent runs. The results were also field tested using INDOT's Laser Profiling vehicle.

Keywords: satellite communications, TCP/IP, spread spectrum radios, inductive and micro-loop detection, vehicle-infrastructure integration.

TABLE OF CONTENTS

LIST OF FIGURES

Figure Page

1. Introduction

1.1. Inductive and Micro-Loop Principle of Operation

Inductive loop detectors are the most widely used sensors in traffic engineering where their primary purpose is vehicle detection. They have also been used in a variety of other applications including vehicle classification [Gajda 2001], vehicle speed estimation along freeways [Lin 2004, El-Geneidy 2004], and travel time estimation by matching vehicle inductive loop signatures taken between widely spaced detector stations [Sun 1999, Oh 2002a, Oh 2002b, Oh 2004]. Microloop detectors are a related technology, which has seen increasing deployment over the past few years. Standard inductive loops and microloops use different physical phenomena for sensing although they operate in a similar fashion from the perspective of roadside electronics, i.e., the same detector cards can be used in some cases.

The classical inductive loop is simply a buried wire loop connected to an alternating current source, which creates an alternating magnetic field. When a vehicle containing electrically conductive material passes over the inductive loop, the magnetic field induces eddy currents in the conductive body of the vehicle, which creates a magnetic coupling between the loop and the vehicle lowering the perceived inductance of the loop. The loop, vehicle and lead-in cable may be modeled as an equivalent inductance in a resonant circuit, which determines the frequency of an oscillator. The presence of a vehicle over the loop is detected by observing a change in resonant frequency caused by the change in inductance[1]. The inductive loop in this capacity has been well studied and there are design guidelines as to how it should be constructed and operated [Klein 2005].

In previous work [Mills 1989], Mills developed a circuit model for the inductive loop, which takes into account the external parasitic capacitances, ground resistances, and the transmission line effects of the cable connecting the loop to the road-side detector. From this model, software was written that accurately calculates the inductance of the loop perceived by the vehicle detection circuitry. The software also computes the loop quality factor. Mills noted that lead-in cable inductance has a significant effect in the overall loop sensitivity. Whereas most of the previous research has gone into characterizing loop performance by accurately modeling its inductance and quality factor, there is little in the literature characterizing the "detection zones" of the loops. This is important for bicycle and small vehicle detection since certain loops exhibit "dead spots" where no detection can take place.

New construction practices now often place the inductive loops approximately 30 cm below the paved surface. Although these installation procedures provide acceptable

[1] Microloops sense the perturbation of the earth's magnetic field caused by the presence of magnetic material in the vicinity of the loop. The microloop sensor translates the magnetic field perturbation into an apparent change in the inductance of the loop as seen by the roadside electronics. Therefore, the same oscillator tank circuit mechanism can be used with both inductive and microloops. One difference is that apparent inductance can only be decreased in a standard inductive loop system while it can either increase or decrease in a microloop system.

detection for trucks and automobiles, their performance with bicycles is less clear. It is well known that octagonal and circular loops have dead spots for bicycle detection. Although there are certain loops which exhibit little or no dead spots for bicycle detection (for example Caltrans Type D [Klein 2005]), the majority of the inductive loops currently in use are either circular or octagonal and hence we focused our study on these loops. For a qualitative comparison between different loops for bicycle detection, the reader is referred to [Wachtel 2000].

1.2. Travel Time Estimation

It is well accepted that travel time information is crucial in a wide range of intelligent transportation applications such as incident detection [Messer 1973, Urbanek 1978], advanced traveler information systems (ATIS) [Tanaka 1994] and the optimization of traffic signals on arterial roads [HCM 2000]. Due to the importance of travel time estimation, several research efforts attempted, over the last two decades, to estimate link travel time [Klein 1997]. Despite these efforts, most practical implementations of travel time estimation have been reduced to the extrapolation of point measures of flow, occupancy, and/or speed (usually obtained from inductive loop detectors used either singly or in pairs as speed "traps"). The inadequacy of these extrapolative approaches has been documented [Dailey 1993] and substantial research efforts have been invested in finding improvements. The research effort on alternative travel time estimation methods may be broadly classified into three subgroups based on traffic models, platoon re-identification or singular vehicle probing. In model-based methods, one estimates travel time by fitting parameters in a traffic-flow model using point measurements [Dailey 1993]. In platoon re-identification methods, travel time is estimated by tracking platoons of vehicles [Coifman 1998]. Probe vehicle travel time estimation methods can be further categorized as:

- Travel time estimation by continuous tracking of an individual vehicle over a video camera's field of view [Kan 1996].
- Travel time estimation by vehicle matching at spaced detector stations using vehicle signatures captured from inductive loops [Sun 1999, Oh 2002a, Oh 2002b, Oh 2004], laser ranging profilers [Kreeger 1996], weigh-in-motion profilers [Christiansen 1996], or license plates [Cui 1997].
- Travel time estimation by direct tracking of individual vehicles using Automatic Vehicle Identification (AVI) tags [Christiansen 1996, Balke 1995, Levine 1994] or cellular phones [Smith 2003].

Among the above classes of methods, probe vehicle methods have resulted in the best performance in travel time estimation. A recurring question in this method has been the characterization of travel time estimation performance as a function of a fraction of the traffic stream [Smith 2003, Turner 1995]. Some studies have reported that acceptable performance results are achievable even in the cases where only a small fraction of the traffic stream is taken into consideration [Coifman 1998]. This is an important finding that ought to be exploited since it states that one can achieve satisfactory travel time estimation performance through a well-chosen subset of the traffic stream. Given that the

penetration of AVI tags or suitably equipped cellular phone infrastructure is still lagging, active investigations in enhancing performance results should focus on improving travel time estimation based on individual vehicle re-identification using signatures from inductive and micro-loop sensors.

1.3. Inductance Signature Based Vehicle Re-identification

Early work on vehicle re-identification and travel time estimation via inductive loop signature matching is contained in the 1999 paper by Sun, Richie, Tsai and Jayakrishnan [Sun 1999]. In this work, vehicle matching between two detector stations, one upstream and one downstream in a "speed trap" setting, is implemented using a feature vector consisting of the following components.

- The maximum value of the raw inductance signature.
- The lane number from which the measurement was captured.
- The speed of the vehicle when the measurement was captured.
- The vehicle's electronic length, which is defined as the product of the vehicle's speed and occupancy.
- A fixed number of samples of an inductive signature waveform.

The last feature in the list above was derived from the raw signature by normalization of the magnitude and rescaling of the abscissa from time to distance using an independent speed measurement. In this framework, all signatures were represented by the same fixed number of samples obtained by re-sampling a spline-interpolated version of the normalized and rescaled raw signatures. Re-identification of vehicles between the two stations was then accomplished by matching feature vectors and travel time was computed for each matched pair of feature vectors (one for an upstream vehicle and one for a downstream vehicle). Assuming that the re-identification is accurate, a histogram of the travel time of the vehicles between the two stations can be generated. Subsequently, several statistics (mean, median, mode) of the travel time distribution are estimated. Sun et al. [Sun 1999] posed the feature vector matching problem as a multi-objective optimization problem, which is solved using a lexicographic ordering of individual objectives. The ordering of individual objectives is used to window the feasible set of potential matches by using the likelihood of re-identified vehicle travel times, the magnitudes of raw signatures, a tolerance window for vehicle electronic length, etc. The authors also introduce five measures of choice (city-block, correlation, similarity, Lebesgue and neural network) to quantify dissimilarity between normalized inductive signatures. The above system was tested in a freeway scenario (SR 25 in Lafayette, CA) and appeared to perform well in regards to travel time estimation, but little data related to the re-identification performance was reported.

Although this work introduced and demonstrated the feasibility of travel time estimation via vehicle detector signatures, it has intrinsic limitations due to the high complexity of the algorithm, which would certainly require extensive calibration in addition to being inapplicable in real-time settings. In fact, in more recent work [Jeng 2006], Ritchie et al. introduce several modifications to the above vehicle re-identification theme to address

the issues related to algorithmic complexity and introduce data compression in the algorithms.

Despite the existence of a substantial volume of work in this area a number of significant issues remain to be fully addressed. Previous methods all depend on the renormalization of the raw signatures. However, this renormalization process is not optimal and could be improved through a more principled approach. Additionally the existence of micro-loop detectors offers the possibility of further performance enhancement, since signatures originating from micro-loop sensors appear to have greater detail as compared to ILD sensors.

2. Problem Statement

This portion of the project studies loop and microloop systems with regard to their detection performance on small vehicles and their capabilities for use with more advanced signature processing algorithms for travel time estimation. Although related by the use of a common technology the detection problem and the signature processing problem are best treated individually.

A. **Design Considerations for Detection of Bicycles Using Inductive Loops.** The problem is to electro-magnetically model the loop detection problem analytically and use a software tool to compute detection zones above a loop with respect to bicycle detection. An experiment will be designed to verify the modeled detection zones using commercially available loop detection hardware. A secondary consideration is to calculate detection zones for differing loop geometries.

B. **Travel Time Estimation by Signature-Based Vehicle Re-identification.** The problem is to derive simple algorithms for loop signature re-identification and then use these algorithms for travel time estimation. A variety of experiments using commercially available loop signature capture devices will be performed to verify the theory. A database will be designed to allow further experimentation.

3. Objectives or Purpose

The objective of this research is two-fold.

A. **Design Considerations for Detection of Bicycles Using Inductive Loops.** The objective is to study loop geometry, loop depth under pavement, loop connection (i.e., series connection or independent connection), and detector sensitivity settings with respect to their effect on the actual detection zone of a small vehicle. The research should result in recommendations on the design of loop detection, which will be useful in situations where small vehicles are of interest.

B. **Travel Time Estimation by Signature-Based Vehicle Re-identification.** The objective is to design algorithms for vehicle re-identification and travel time

estimation and test them in a field scenario using commercially available loop signature capture devices.

4. Work Plan

The work of this project was carried out in two major tasks described below. Since the tasks were essentially independent of each other, they will be described separately in this section and the next.

4.1. Task A: Design Considerations for Detection of Bicycles Using Inductive Loops

The following work was completed. Results are reported in the next section.

1. Develop circuit and electro-magnetic models for the loop detection problem.
2. Identify appropriate numerical electro-magnetic modeling software.
3. Verify and calibrate numerical model using field measurements.
4. Carry out numerical experiments characterizing the detection zone for bicycle detection.

4.2. Task B: Travel Time Estimation by Signature-Based Vehicle Re-identification

The following work was completed. Results are reported in the next section.

1. Develop data collection hardware and software for capturing inductive and micro-loop signatures and comparing to video ground truth.
2. Design an appropriate database for storing signatures, image frames, and results of vehicle re-identification.
3. Design algorithms for signature-based vehicle re-identification.
4. Test the algorithms and store the results in the database.
5. Design algorithm for travel time estimation.

5. Analysis of Data

5.1. Task A: Design Considerations for Detection of Bicycles Using Inductive Loops

5.1.1. Loop Detector Technology

The goal of the loop detector is to measure the relative change in inductance of the inductive loop $(\Delta L / L)$, also called loop sensitivity (S), when a vehicle is present. This, however, is hard to measure directly. Typically, the inductive loop forms part of a tuned oscillator circuit [Klein 2005] that has a resonant frequency of the form

$$f = KL^{-\frac{1}{2}}$$

where K is a proportionality constant. The above equation is accurate only for a coil having a high quality factor. Most practical inductive loops have this property.

The presence of a vehicle over a loop causes a small reduction in the perceived inductance L, which results in an increase in the resonant frequency. Let $\Delta L = L_{nv} - L_v$ and $\Delta f = f_v - f_{nv}$, where subscripts *nv* and *v* correspond to the variables in the absence and presence of a vehicle, respectively. Then

$$\begin{aligned} f_v &= K(L_{nv} - \Delta L)^{-1/2} \\ &= f_{nv}(1 - \Delta L / L_{nv})^{-1/2} \end{aligned}$$

where $f_{nv} = KL_{nv}^{-1/2}$. It can be shown that

$$\frac{\Delta f}{f_{nv}} = \frac{1}{\sqrt{1 - \Delta L / L_{nv}}} - 1$$

For small $\Delta L / L_{nv}$ using the first two terms of the Taylor series expansion results in the following approximation relating the loop sensitivity to the relative frequency shift:

$$\frac{\Delta f}{f_{nv}} \approx \frac{1}{2}\frac{\Delta L}{L_{nv}} = \frac{1}{2}S$$

This is the detection strategy around which most modern detectors are based as it is much easier to measure a change in frequency. In general this is done by measuring frequency shifts, ratios of frequency shifts, period shifts, or ratios of period shifts [Klein 2005].

Typical values for $\Delta L / L_{nv}$ range from 2.5×10^{-5} to 6.4×10^{-3} [Reno 2004]. For a nominal oscillator loop frequency of 50 kHz this implies a frequency change of 1.2 Hz to 320 Hz. It can be seen that sensitivity at the lowest setting is a reasonably difficult detection problem.

5.1.2. System Model

In choosing a model for the bicycle, the frame of the bicycle is assumed to be made up of a lightweight non-conducting material (like carbon fiber) and thus the only major conducting parts are the wheels. Even composite wheels have a circumferential metal band that brake pads use to contact the rim. This represents the worst case scenario for bicycle detection, since the addition of a conducting frame increases the detection sensitivity. We first model a single wheel of the bicycle by a circular conducting filament. The loop sensitivity in this unicycle model can be determined by simple circuit analysis. Superposition of results from the unicycle model can be used to determine the loop sensitivity for the bicycle $\Delta L / L_{nv}$. The inductive loop is modeled by a perfect conductor. This represents the best case for the detector. Additional parasitic effects (e.g., ground, reinforced steel) only degrade the sensitivity of the loop detector.

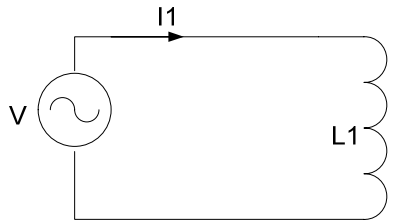

Figure 1: Model of Loop Detector.

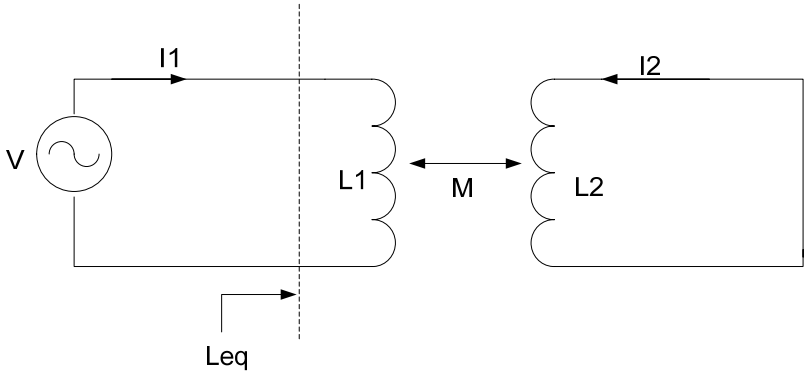

Figure 2: Model of Loop Detector with Unicycle Interactions.

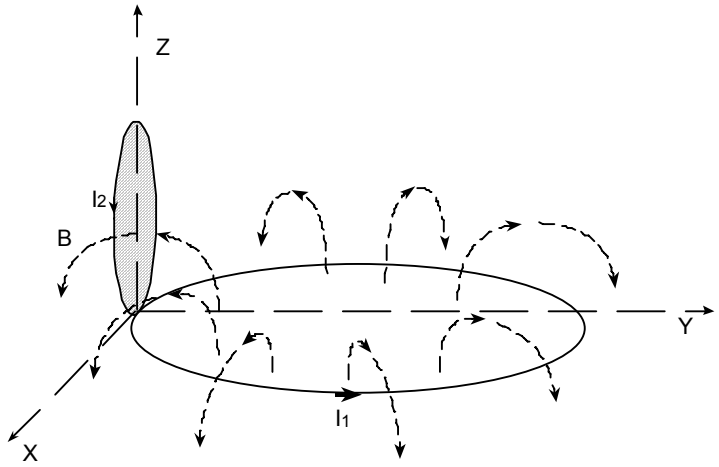

Figure 3: Magnetic Flux Linkage between Loop Detector and a Unicycle Wheel.

From circuit theory, it can be shown that the relative change in inductance of the loop detector is

$$\frac{\Delta L}{L_1} = \frac{M^2}{L_1 L_2}$$

Recall that the self inductance of a loop having N_1 turns is

$$L_1 = \frac{N_1 \int \mathbf{B}.\mathbf{ds_1}}{I_1},$$

where **B** is the magnetic flux density and I_1 is the current flowing through the loop. L_1 is thus obtained by calculating the flux linkage, using a surface integral between **B** and the surface enclosed by the loop. The mutual inductance is given by

$$M = \frac{N_2 \int \mathbf{B}.\mathbf{ds_2}}{I_1},$$

where the surface integral is evaluated over the surface enclosed by the wheel. An example of the magnetic flux linkage between the loop detector and bicycle wheel is shown in Fig. 3. The magnetic flux density is determined by the method of finite moments using the Numerical Electromagnetic Code NEC-2 software [NEC]. This software allows one to specify the loop geometry along with wire dimensions, and it determines the resulting magnetic flux density at a specified grid in free space. The surface integrals are calculated by numerical integration using MATLAB©.

The above set of equations allows the calculation of loop sensitivity for a unicycle wheel centered at any specified point in free–space allowing us to study the effect of increasing the separation between the loop below the pavement and the unicycle wheel.

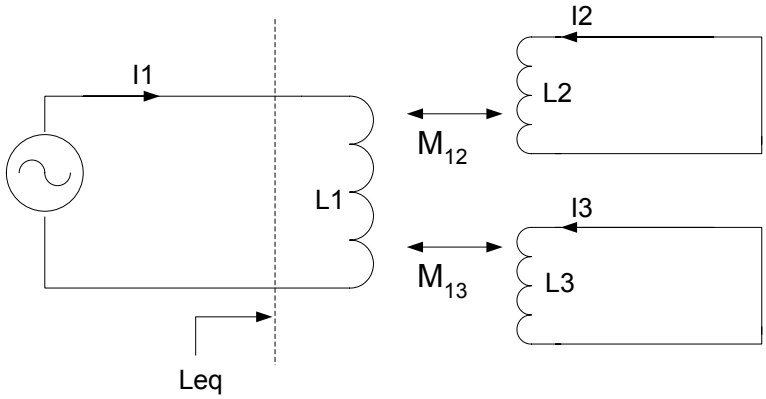

Figure 4: Circuit model for bicycle-loop interaction.

The loop sensitivity for the bicycle can be computed using the circuit model shown in Fig. 4**.** Using circuit analysis, it can be shown that the loop sensitivity is given by

$$\frac{\Delta L}{L_1} = \frac{M_{12}^2}{L_2 L_1} + \frac{M_{13}^2}{L_3 L_1}.$$

Each term on the right hand side corresponds to the sensitivity of the loop in the presence of a unicycle. Superposition of the unicycle sensitivity calculations gives us the sensitivity of the loop for a bicycle.

So far, we have discussed the sensitivity of a single loop in the presence of a vehicle. Typically, multiple loops are used to detect vehicle presence. They can be either connected in series to a single road-side detector or each loop can be connected to its own loop detector. From our simulations we have observed that with the geometry of a typical

loop placement with four 1.8 m × 1.8 m loops spaced 4.5 m on center**,** the bicycle interacts with only one loop at a time. The mutual inductance between the bicycle and the rest of the loops can be ignored. In the series connection case, the sensitivity scales down with the number of loops connected in series, since the overall inductance connected to the detector is the sum of the inductances of the individual loops.

5.1.3. Simulation Results

5.1.3.1. Experiment 1 – Model Verification

To verify the correctness of our model, loop sensitivities predicted from our model are compared with measured loop detector data. The loop sensitivity measurements are made with a copper wire of radius 30 cm having a thickness of 3 mm using a Reno loop detector [Reno 2004]. The frequency at which the loop is excited is 47 kHz. The measured data corresponds to the unicycle at ground level. The expected depth of the buried loop is between 4 cm to 7 cm, but the exact depth cannot be verified without destructively coring the pavement. The copper wire model removes the dependence of the results on the particular bicycle make/model used and the results can be easily reproduced or validated. Bicycle wheels have variability in their widths and sizes resulting in variable detection performance. The goal of our research is to deduce the shapes of the detection zones based on simple theoretical models as we change the loop configuration parameters (e.g., differing depths and wiring). The theoretical model uses a perfect conductor assumption and hence the copper wire loop is used to verify the theoretical predictions. The conclusions drawn hold for real bicycle wheels.

We compare the loop sensitivity for a unicycle and octagonal and circular inductive loops at different cross-sections with both simulated and measured data. The calculation of the simulated data takes into account lead-in inductance, which is about 0.22 μH/ft [Mills 1989]. Simulations are performed for different loop depths below the ground. The results are shown in Fig. 5. It was observed that a depth of 5 cm provides the closest fit to the measured data.

We note that, even though the lack of knowledge of the depth creates an uncertainty in the exact sensitivity, there is a general agreement between the shapes of the measured and simulated results.

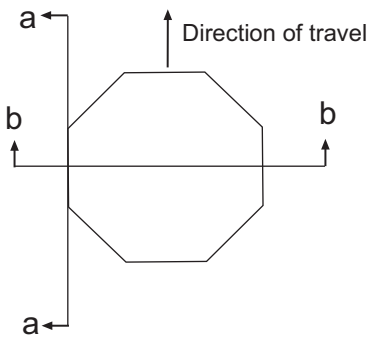

a) 1.8 m x 1.8 m octagonal detector

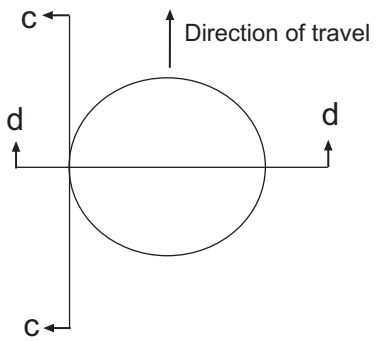

b) 1.8 m diameter circular detector

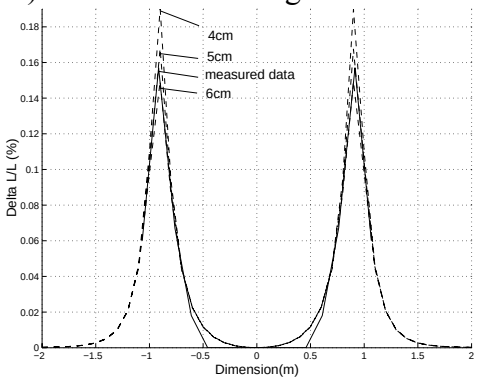

c) ΔL/L for cross-section b-b

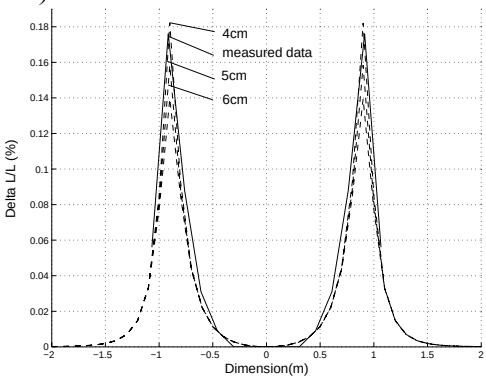

d) ΔL/L for cross-section d-d

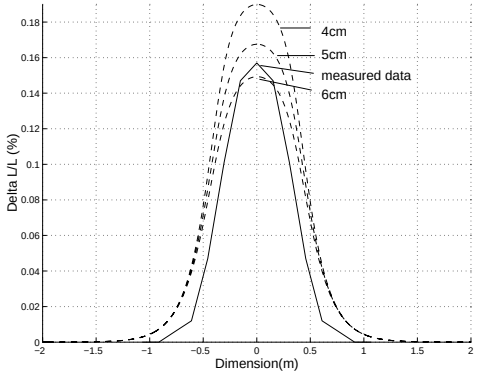

e) ΔL/L for cross-section a-a

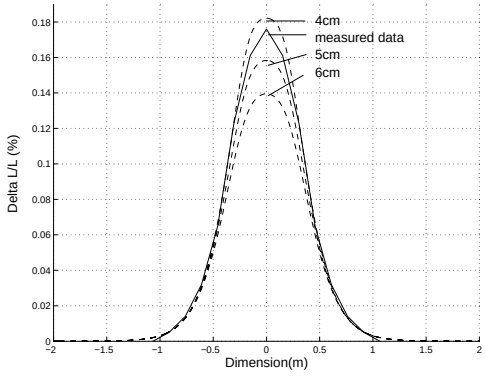

f) ΔL/L for cross-section c-c

Figure 5: Modeled vs. Observed. Relative change in inductance for octagon and circular loop. Lead in inductance included.

5.1.3.2. Experiment 2 – Circular versus Octagonal Loop Sensitivities for Unicycle

From Fig. 5, the sensitivities of the octagonal and circular loops for unicycle detection are nearly the same. The shapes of the detection zones indicate that octagonal and circular loops have nearly identical performance in terms of unicycle detection. This is illustrated in Fig. 6, where we show sensitivity contour plots at a loop depth of 9 cm. These plots are in very close agreement for a variety of sensitivity settings. Note that, for this comparison, the lead-in inductance is not taken into account since it varies depending on the distance between the loops and the loop detection box.

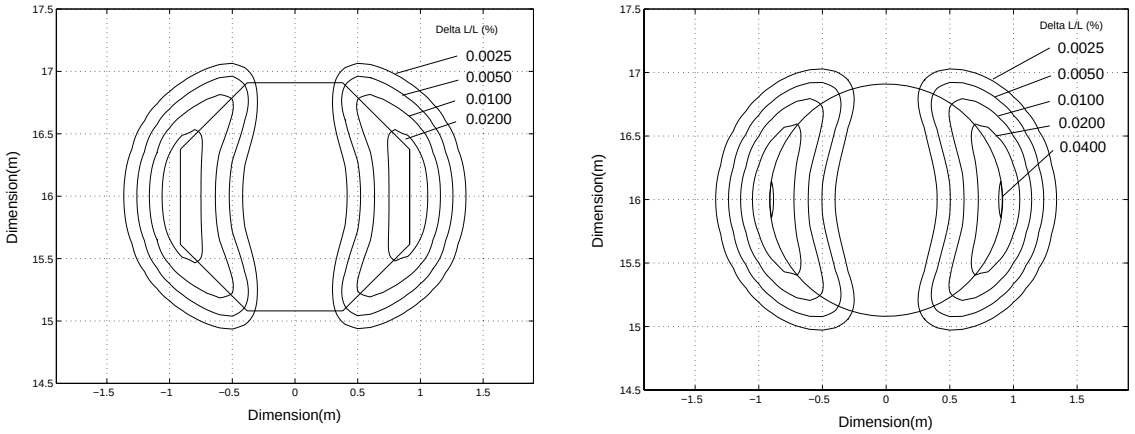

a) 1.8 m x 1.8 m octagon at depth 9 cm. b) 1.8 m diameter circle at depth 9 cm.

Figure 6: Detection zone for varying ΔL/L sensitivity for a three-turn loop detecting a unicycle without a lead-in inductance.

5.1.3.3. Experiment 3 – Bicycle Detection

The bicycle is modeled by two unicycles with a center-to-center separation of 1 m. The objective is to study the bicycle detection zones for standard sensitivity setting ($\Delta L / L$ of 0.02 %) [Klein 2005]. A placement of four 1.8 m $\times$ 1.8 m octagonal loops spaced 4.5 m on center and connected in series is used for this purpose. Fig. 7 shows the detection zone. A bicycle positioned between the two loops, or placed too close to the road markings on both sides of the lane, or positioned in the center of the lane will go undetected. Clearly, there are considerable dead spots both inside and between the loops, showing a dismal performance for the default sensitivity setting.

Next, we tested the difference between the circular loop and the octagonal loop. Fig. 8 shows the sensitivity contours for both octagonal and circular loops at the default sensitivity. It is seen that there is not much difference in terms of detection zone between the two. The octagonal loop has a slightly wider detection zone, while the circular loop has a slightly longer zone. Nevertheless, the difference is minute and it can be safely assumed that both the loops will perform identically in real road conditions.

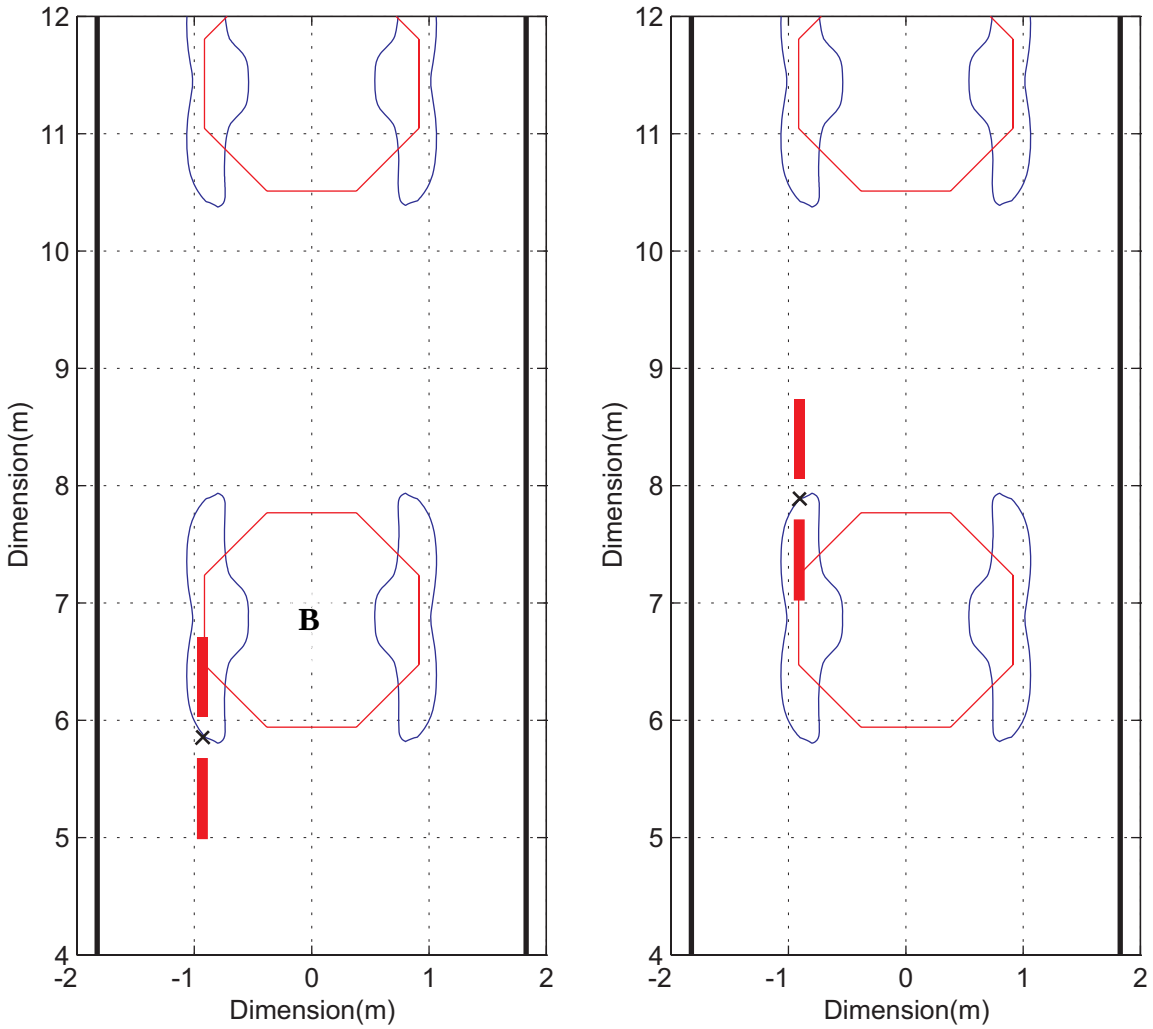

a) Detection zone contour of ΔL/L at 0.02% with four loops connected in series. A bike is shown entering loop B.

b) Detection zone contour of ΔL/L at 0.02% with four loops connected in series. A bike is shown leaving loop B.

Figure 7: Sensitivity contour for ΔL/L threshold of 0.02% for 1.8 m x 1.8 m octagon.

5.1.3.4. Experiment 4 – Series versus Independent Connection

Here the effect of connecting the loop in a series connection is compared to connecting them independently. Fig. 9 shows the detection zones for series and independent connections. It is observed that an independent connection has a much larger detection zone than that of a series one. Since the total inductance of the series connection is four times that of the independent connection, the sensitivity is reduced by the corresponding amount, for a given change in ΔL .

Fig. 10 shows the maximum depth that these loops can be buried beneath the surface pavement before their detection zones almost disappear. This shows that an increase in the depth of the loop to only 14 cm, can even cause a significant degradation in the

detection zones for the series connection. Again, the maximum depth of the independent connection significantly exceeds that of the series one. It can be seen that there is a significant advantage in using a fully independent loop connection when detecting bicycles. However, other factors such as cost and maintenance might prevent this from being widely implemented. It is proposed that one independent detector be used at least for the first loop nearest to the traffic light, where the lane discipline is dismal. The series connection could then be used for the rest of the loops.

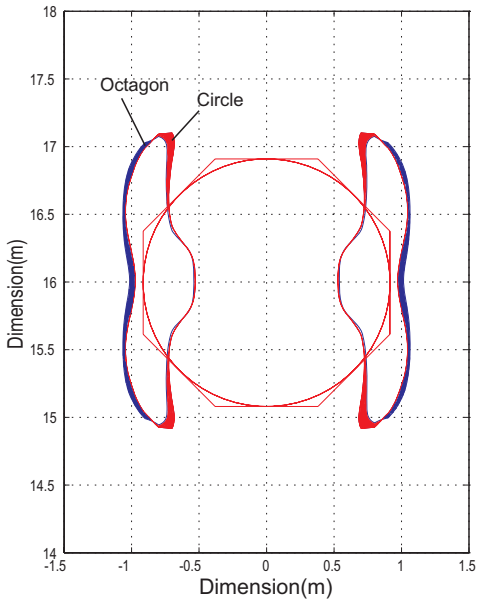

a) Loops connected in series.

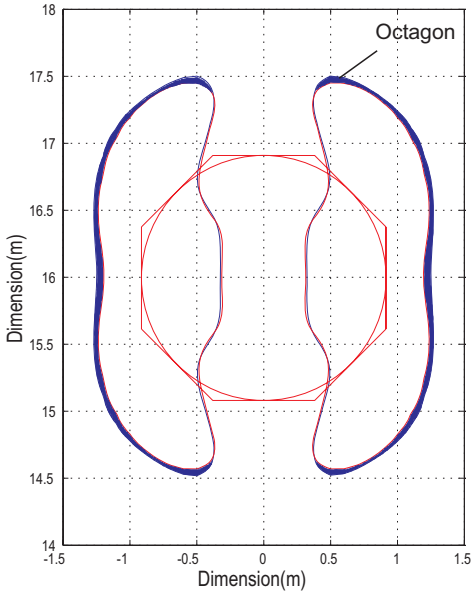

b) Loops connected independently.

Figure 8: Comparison of detection areas between circular and octagonal loops via sensitivity countour for ΔL/L threshold of 0.02%.

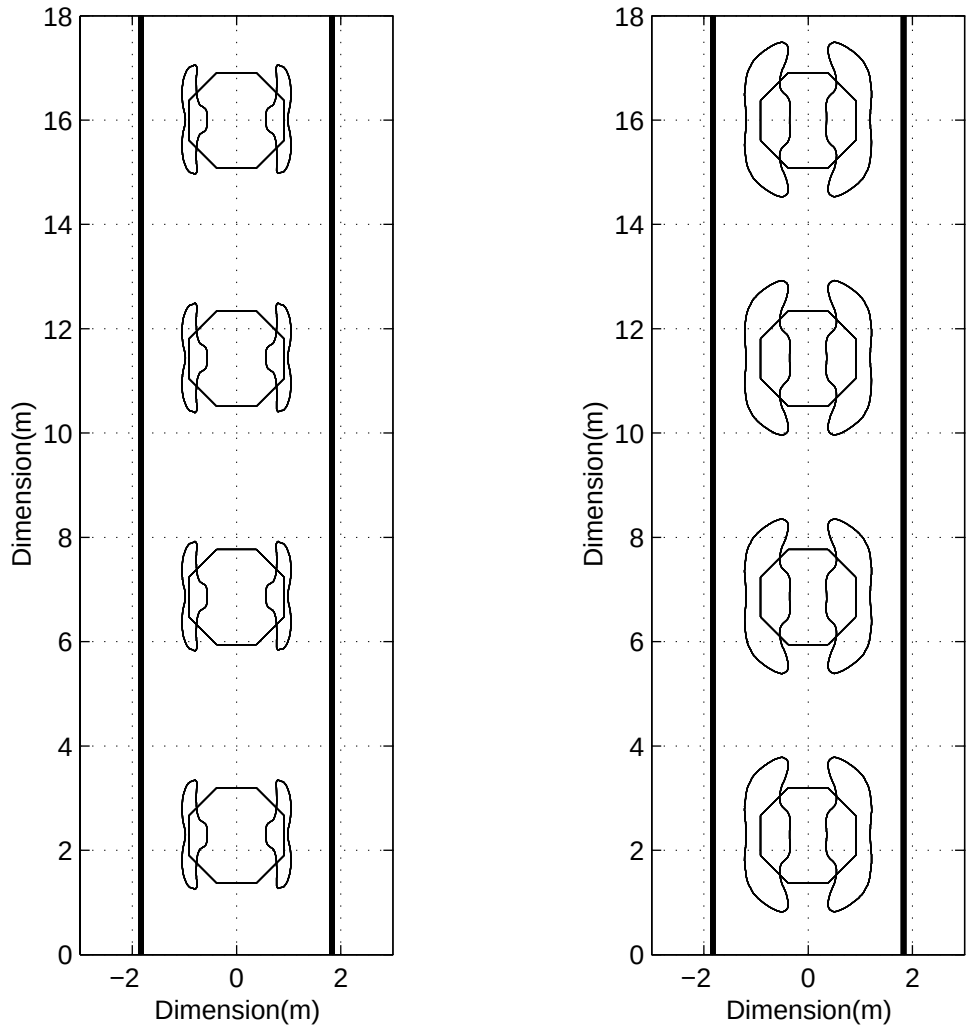

a) Loops connected in series. Octagon depth 5 cm.

b) Independent loop detectors. Octagon depth 5 cm.

Figure 9: Sensitivity contour comparison between series and independent wiring for the octagonal loop with lead-in inductance. The depth of the loop below the ground is fixed. ΔL/L threshold is 0.02%.

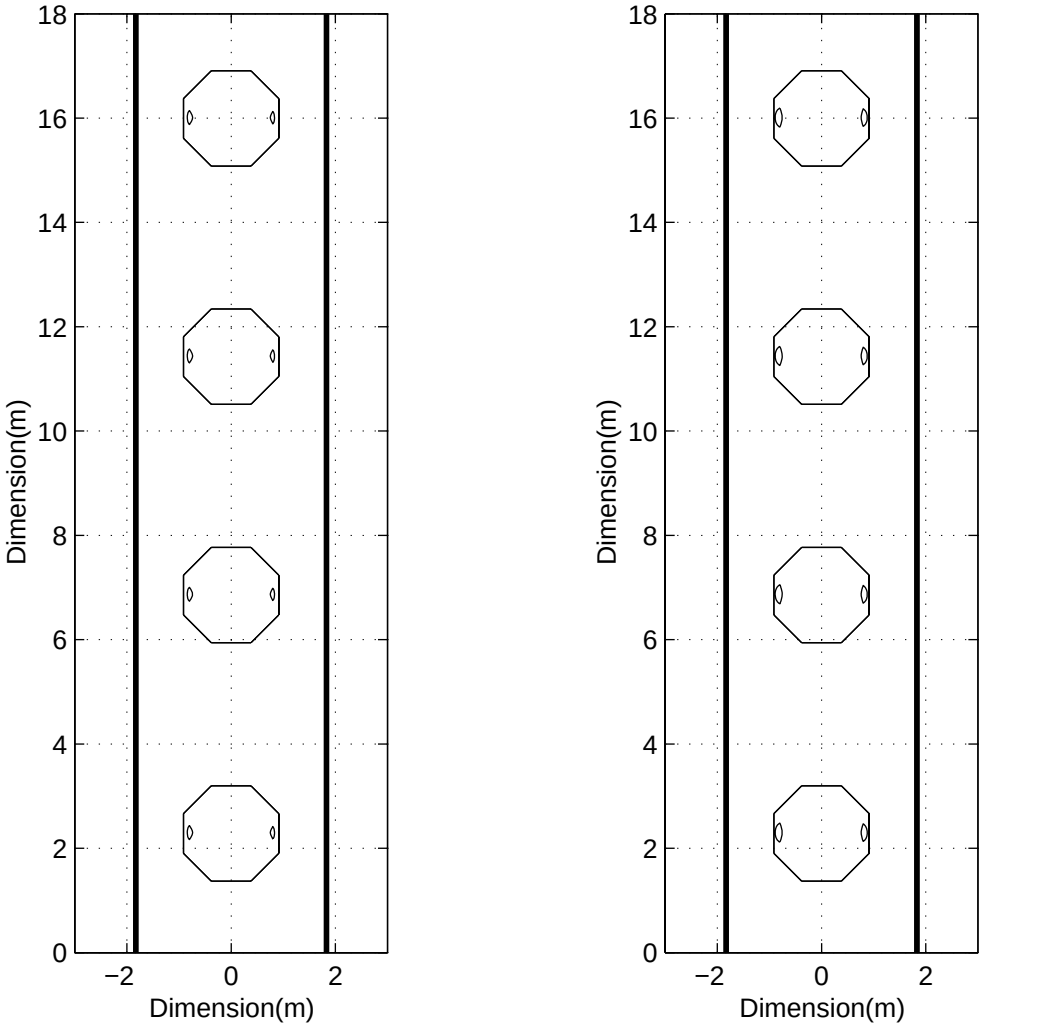

a) Loops connected in series. Octagon depth 14 cm.

b) Independent loop detectors. Octagon depth 41 cm.

Figure 10: Comparison of maximum depth of operation for series and independently wired octagonal loops with lead-in inductance. ΔL/L threshold is set to 0.02 %.

5.2. Task B: Travel Time Estimation by Signature-Based Vehicle Re-identification

5.2.1: Data Collection Hardware and Test Sites

For the validation of our work two data collection experiments have been devised. First, a single speed trap consisting of two loops spaced close together; and second, a dual speed trap created by two traps that are a significant distance apart. Single speed trap tests were conducted at the intersection of Stadium Avenue and US 231 in West Lafayette, IN where micro loops and inductive loops were both analyzed. Additional tests

were performed at mile marker 128 (MM128) on I-65 Northwest of Indianapolis, IN, where all data was collected under free flowing conditions.

At a data collection site the loops in each speed trap are connected to a two channel detector card, which is then connected to a laptop using manufacturer supplied software to record the Δf/f waveform from each loop. Δf/f is a percentage measurement of the change in the oscillation frequency of a loop relative to the oscillation frequency when there is nothing over the top of the loop. Also at each site, video cameras showing the speed traps, with a timestamp overlay that is synchronized to the laptops, are recorded onto DVDs and used to determine ground truth for the data set. Once the Δf/f waveforms from each trap have been processed, the Δf/f signature of each vehicle, along with a picture of the vehicle, is loaded into a database for analysis (Figure 11b).

At the US 231 site (Figure 11a), data is collected as vehicles pass over the inductive trap (NB8, NB6) and the micro trap (NBM7, NBM5), with each loop pair having a spacing of 22 feet. The data collected from the inductive loops is sampled at 83.3 Hz, while the micro loops are sampled at 200 Hz. The MM128 site consists of two lanes in each direction, with data being collected from micro loops in the north bound passing lane. The micro-loops are 20 feet apart and are sampled at 100 Hz. The variation in sampling rates is due to various settings of the detector cards at the different installations, as well as differences between manufacturers.

A trap scenario is simulated at the US 231 location by using the NBM7, NBM5 trap in conjunction with the NBM2, NBM1 trap. The spacing between the first loops in each trap is approximately 150 feet. The data from each trap is collected independently and then combined during the analysis of the data set. Although in an ideal arrangement, setback loops similar to NAM7/NAM5 and NBM7/NBM5 would be installed at adjacent intersections.

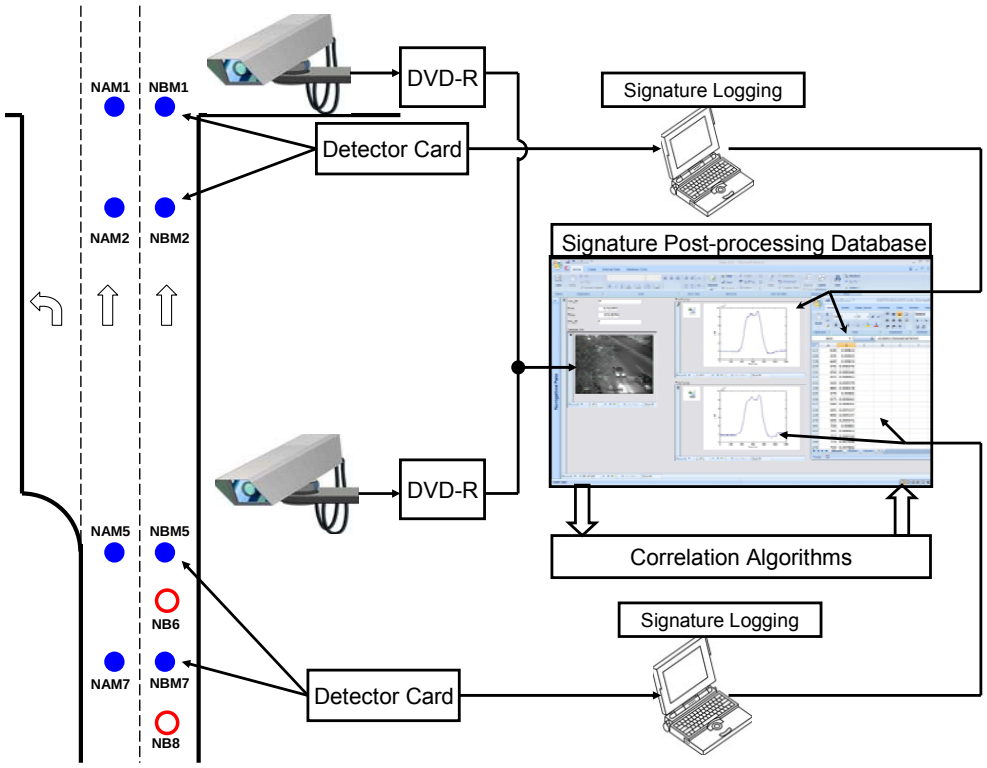

a)Signature logging and post-processing block diagram

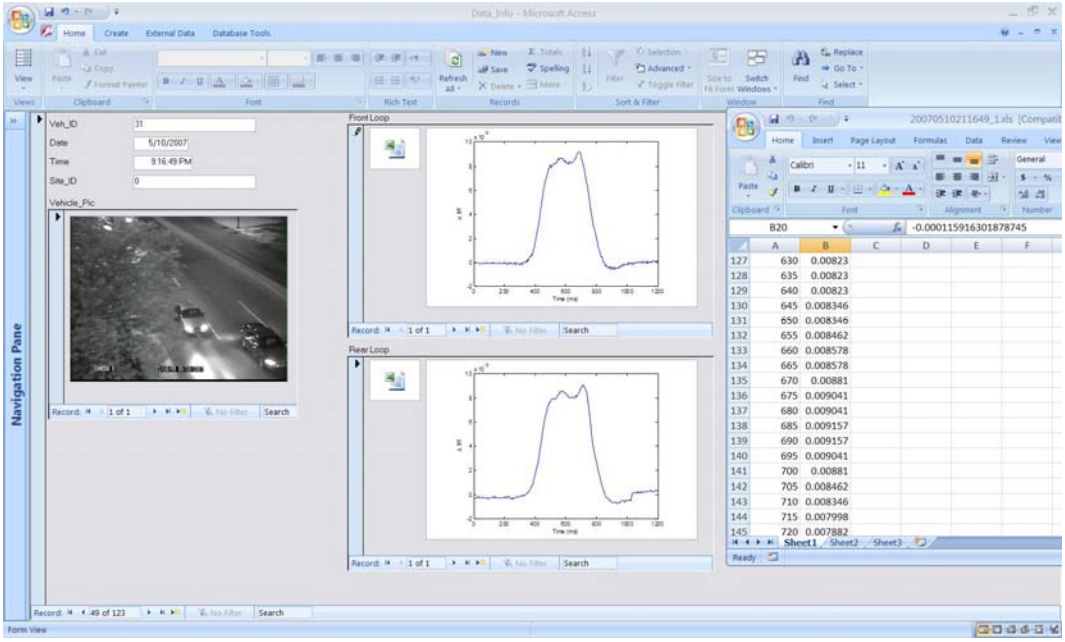

b) Screenshot of Access 2007 post-processing database.

Figure 11: West Lafayette site signature logging and post-processing block diagram.

5.2.2: Signal Processing

5.2.2.1: Signature Detection and Segmentation

Traditionally signature matching algorithms have relied on proprietary signature detection and segmentation packages (call functions) which are not necessary optimized for signature re-identification applications. Vehicle detector call functions are designed to minimize the probability of missing a passing vehicle. An approach better suited for signature matching applications is a call function that discards low energy or noisy waveforms while adequately selecting the waveforms which have a higher probability of re-identification.

For this work a call function was designed by casting the signature segmentation problem as a detection problem in the presence of uncertainties. Under the absence of a vehicle over the detector, the sampled detector output x(n) is modeled as a Gaussian noise process w(n). When a vehicle is present over the loop, the sampled detector output is represented the sum of an unknown discrete waveform s(n) with additive Gaussian noise. The hypothesis testing problem to solve is:

$$H_o: \; x(n) = w(n) \qquad \text{versus} \qquad H_1: x(n) = s(n) + w(n)$$

Devising a Generalized Likelihood Ratio Test with the appropriate threshold, we generate a call function with the properties mentioned above. After the detection and segmentation of "good" signatures in the traffic stream, we proceed to the signature normalization procedure.

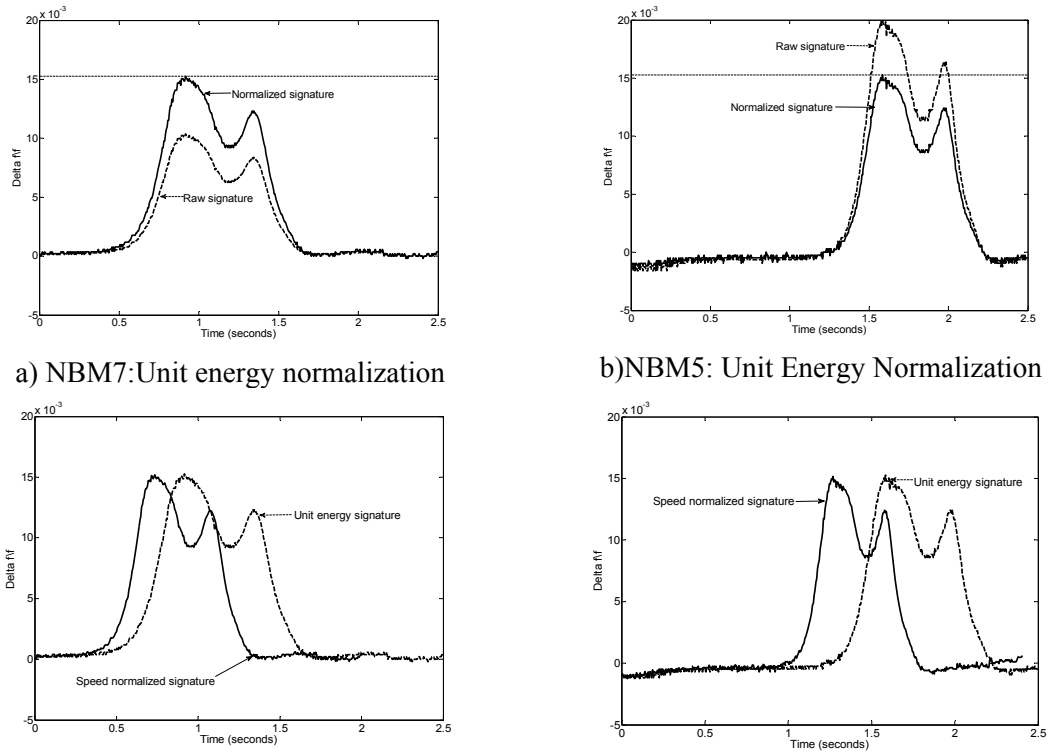

a) NBM7:Unit energy normalization

b)NBM5: Unit Energy Normalization

c)NBM7: Speed Normalization (20mph to 30mph)

d)NBM5:Speed Normalization (20mph to 30mph)

Figure 12: Unit Energy and speed normalization of signatures.

5.2.2.2: Signature Normalization

Signatures at the upstream station (NBM5, NBM7) and signatures at the downstream station (NBM1, NBM2) are connected to different detector cards and have different level settings, noise characteristics, etc. Therefore it is necessary to renormalize all collected raw signatures (upstream and downstream) to a common reference prior to the signature matching procedure. For the purpose of our signature matching procedure (formulated in the following section), it is sufficient to normalize all raw signatures to have unit energy (and not the maximum value as done in [Sun 1999]). The energy normalization procedure is illustrated in Figures 12a and 12b. The next step in the normalization process is to correct for the speed variations of a traveling vehicle between the upstream station and the downstream station. This process consists of transforming all signatures to a common nominal speed V_o. The speed normalization enables one to ensure that the speed of vehicles between the two stations is not being matched. Under free-flowing conditions, it is fair to assume that a traveling vehicle passes across the two loops at a given station at a constant speed. The presence of two detectors at each station allows one to compute the speed V_u of the vehicle upstream and the speed V_d of the vehicle downstream.

Using multi-rate signal processing techniques, it can be demonstrated that the signature from a detector corresponding to a vehicle traveling at speed V_u is simply a fractionally

resampled version of the signature corresponding to the same vehicle traveling at the nominal speed V_o.

The procedure has been experimentally observed in [Park 2007] where the same vehicle has been driven over the same ILD detector at different speeds and the compression/dilation effect of the signatures as a function of speed was noted. In Figures 12c and 12d, the speed normalization was illustrated using real data and the nominal speed (V_o) of 30 mph. An illustrative diagram outlining the step-by-step procedures of the entire signature normalization process (energy and speed normalization) is presented in Figure 13.

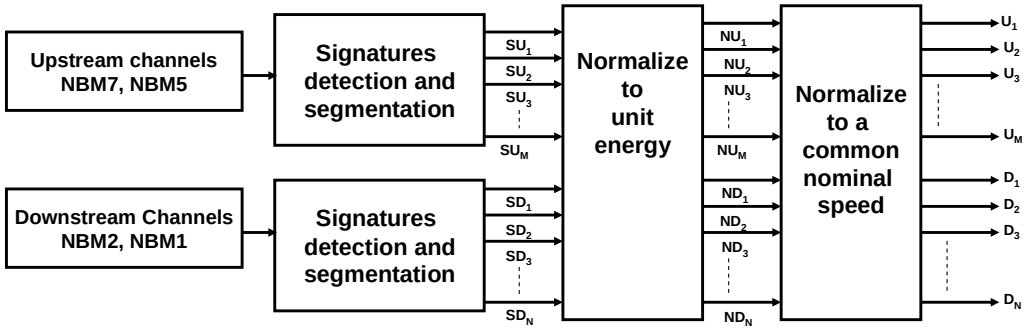

Figure 13: Collected data post-processing diagram.

5.2.3: Matching Vehicle Signatures

After normalization, all processed signatures (from the upstream and downstream stations) have unit energy and are optimally transformed to a reference of a common nominal speed. There is then an adequate and simple framework to apply the signature matching algorithm. The signature matching problem is formulated using techniques from communication theory (e.g., maximum a-posteriori probability detection). A vehicle's processed signature is analogous to a baseband pulse that is used to carry information in a communication system. In this context the optimal receiver consists of a bank of matched filters (correlators). In this specific context, there is a set of processed signatures from a detector located at the upstream station (e.g., NBM7 in Figure 11), and one wishes to match to each processed signature acquired downstream (e.g., NBM1 in Figure 11) the upstream signature that comes from the same vehicle. The optimal procedure using the MAP classifier mentioned above is the following:

- Given a downstream acquired and normalized signature, a cross-correlation function is generated with all normalized signatures from the upstream detector.
- For each cross-correlation function, the corresponding maximum value is recorded.
- Each downstream signature is assigned the upstream signature which has the largest maximum value of the cross-correlation function.

- The process is repeated for each acquired signature from the downstream detector.

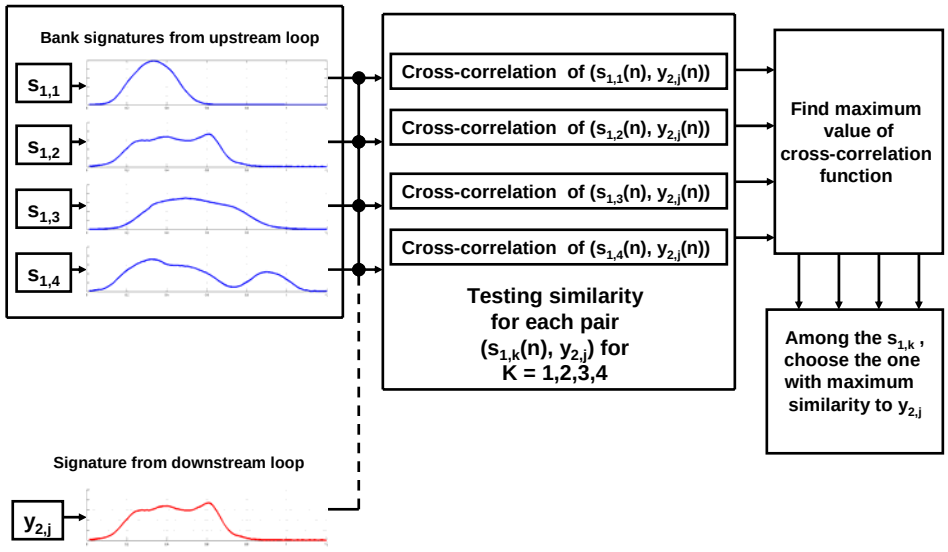

Figure 14: Maximum a-posteriori (MAP) classifier architecture for implementing a minimum probability of error matching of a downstream signature to a collection of candidate upstream signatures.

The above algorithm minimizes the probability of mismatches and the Maximum A-Posteriori (MAP) classifier architecture for implementing a minimum probability of error matching of a downstream signature to a collection of candidate upstream signatures is illustrated in Figure 14. In the above algorithm, the operation of cross-correlation prior to computing the maximum can be interpreted as an alignment of the downstream signature with the upstream signature and then computing their similarity. The similarity is quantified by the inner product between the aligned signatures. Therefore the probability of mismatches is smaller when the vehicle detector used generates signatures with high level of dissimilarity from vehicle to vehicle. For typical vehicles a micro-loop detector produces signatures that are richer in detail as compared to the signatures generated by an ILD. This is seen in Figure 15 where a typical vehicle is shown with its corresponding ILD and micro-loop signatures. For atypical vehicles (i.e., large trucks) both the ILD and the micro-loop signatures have sufficient detail as shown in Figure 16. To further illustrate the advantage of the micro-loop detector over the ILD detector for this signature-matching algorithm, we show in Figure 17, the histogram of the maximum cross-correlation between upstream and downstream vehicles when using an ILD detector (Figure 17a) versus a micro-loop detector (Figure 17b). The maximums of the cross-correlations for ILD signatures are very high in general and their distribution has a

smaller variance as compared to micro-loop signatures. This is an indication that it is more difficult to discriminate vehicle signatures that come from an ILD. Therefore when choosing a detector for signature matching applications, it is preferable to opt for micro-loop sensors. Additionally it has been observed that atypical signatures (i.e., large trucks) can be easily discriminated from one another. Therefore when a large number of atypical signatures are present in the data, it is advisable to base the signature matching procedure solely on this subset of signatures.

The next section will show that this has been found to greatly improve performance. The choice of adequate sensors and signature subsets, and the use of the proposed MAP classifier, provide the necessary conditions for a computationally efficient and robust travel time estimation scheme.

a)Vehicle generating signatures

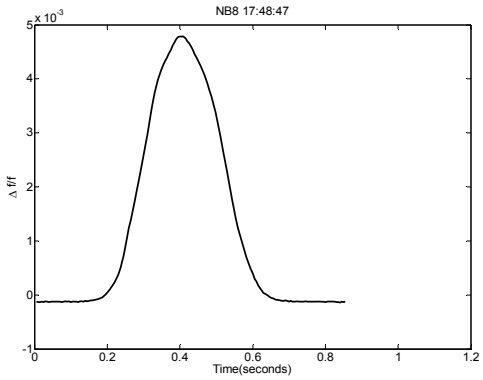

b) NB8:Typical ILD signature

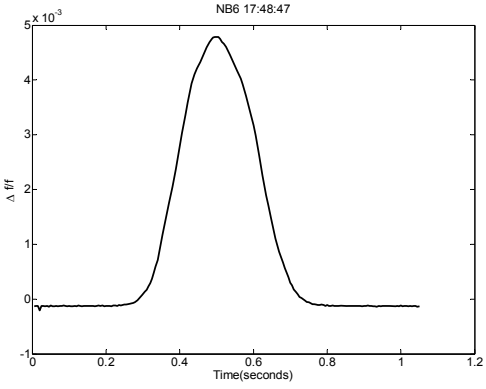

c)NB6: Typical ILD signature

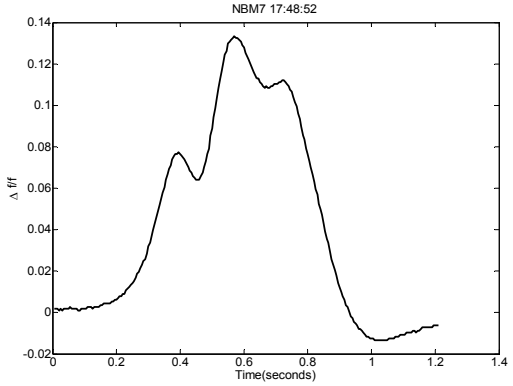

d) NBM7: Typical Microloop signature

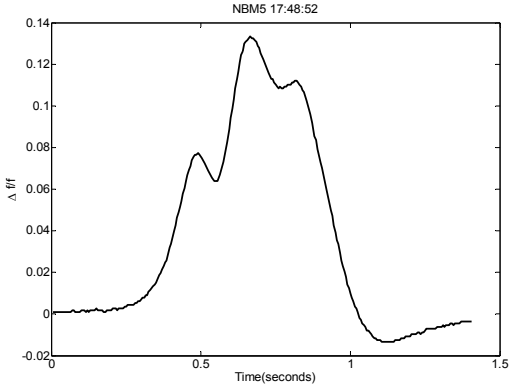

e) NBM5: Typical Microloop signature

Figure 15: Typical processed signatures of a passenger car
NB8-NB6 correlation value: 0.99985
NBM7-NBM5 correlation value: 0.9938.

a) Vehicle generating signatures

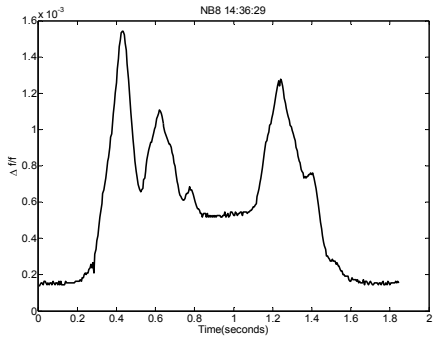

b) NB8:Typical ILD signature

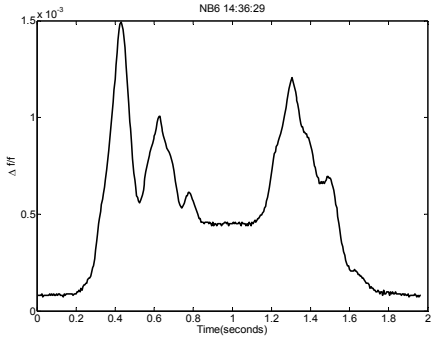

c)NB6: Typical ILD signature

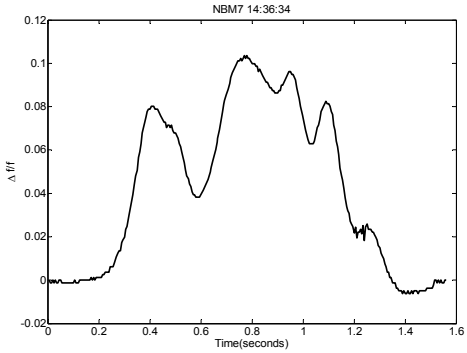

d) NBM7: Typical Microloop signature

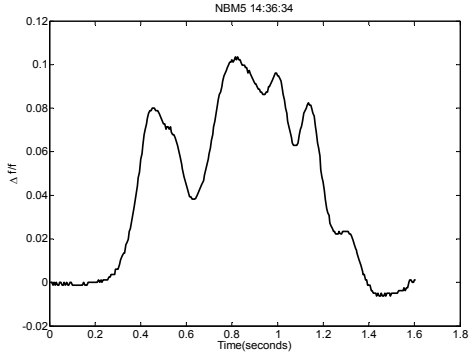

e) NBM5: Typical Microloop signature

Figure 16: Typical processed signatures of a large truck
NB8-NB6 correlation value: 0.99317
NBM7-NBM5 correlation value: 0.97843.

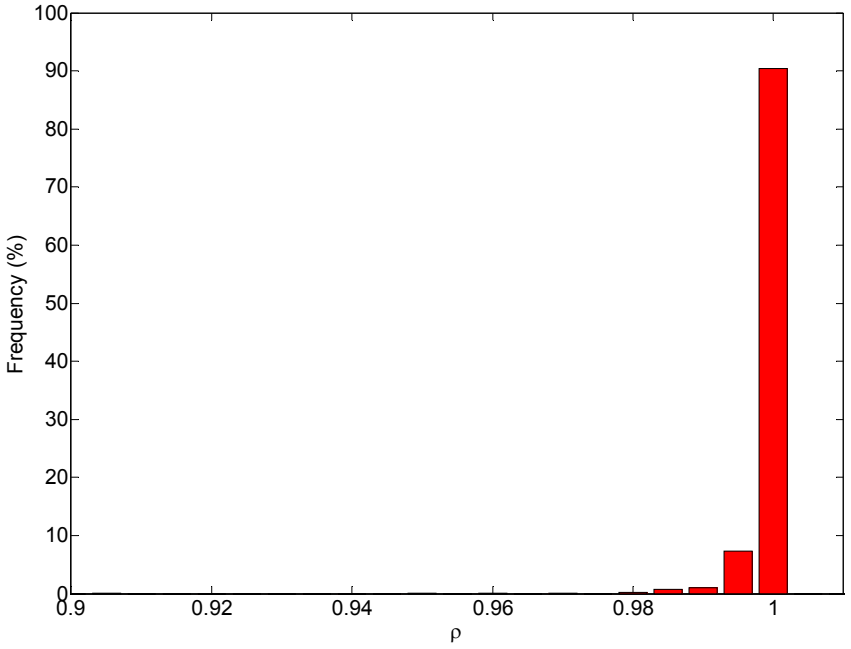

a) Histogram of ILD signatures correlation values

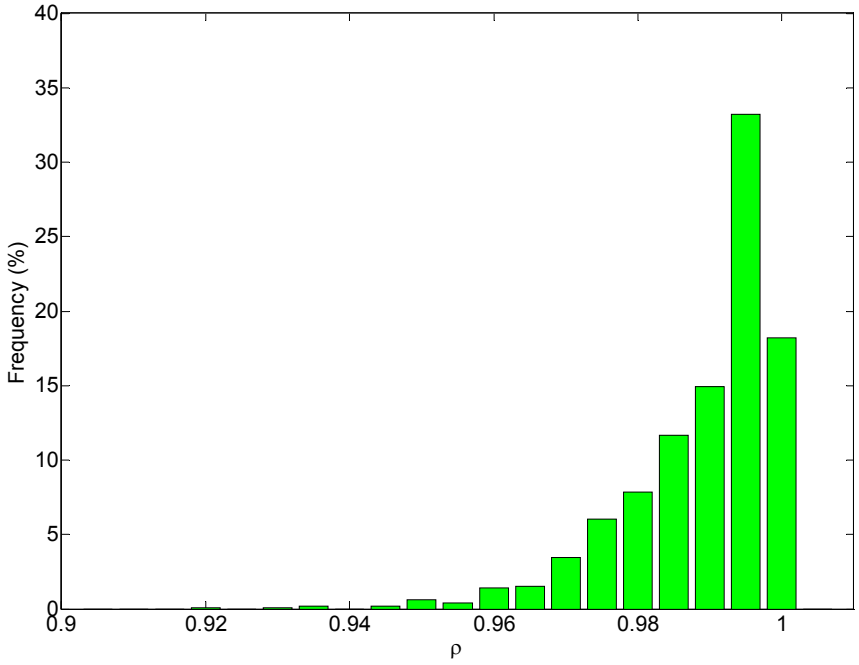

b) Histogram of micro-loop signatures correlation values

Figure 17: Histogram of correlation values for ILD and microloop signatures.

5.2.4: Travel Time Estimation

The outputs of the vehicle signature matching algorithm are pair-wise assignments between the set of upstream signatures and the set of downstream signatures. For each pair the corresponding travel time is calculated, which can be used to filter out some assignments that correspond to false re-identifications. Matched pair-wise assignments with negative travel times can be discarded since these assignments are physically infeasible (i.e., feasibility constraint). Given the length of the road section between the upstream station and the downstream station, some travel times can be found to be very unlikely and the corresponding pair-wise assignments removed from the set (i.e., likelihood constraint).

The histogram of the remaining pairs of upstream-to-downstream assignments (assuming a sufficiently large set) constitutes an estimation of the distribution of the travel time of vehicles over the road section. The travel time over the road section is estimated as the mode of the filtered histogram (after likelihood and feasibility windowing), which is the most likely travel time of vehicles on the road during the considered time span. An illustration of the travel time generation procedure is given in Figure 18.

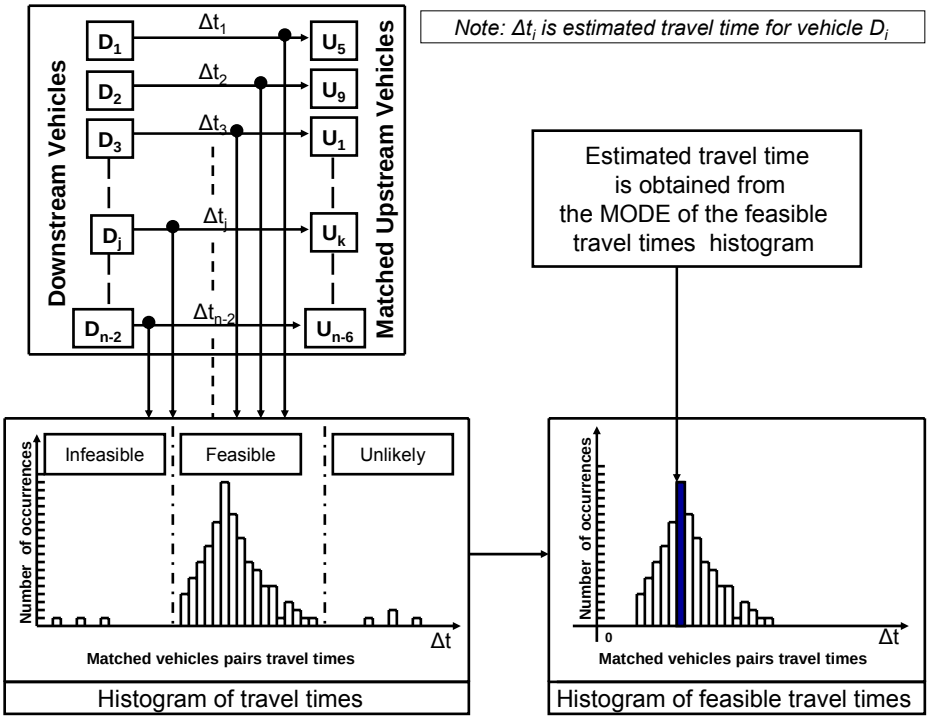

Figure 18: Illustration of travel time generation procedure.

5.2.5: Travel Time Estimation Results

In the first experiment (MM128), the performance of the algorithms under free flowing traffic is considered. A "speed trap" was implemented by using upstream and

downstream stations that were separated by only 20 feet. Performance results from this simple scenario are transferable to more realistic scenarios, since the proposed pre-processing procedure and signature matching algorithm is independent of the distance separating the upstream and the downstream station when feasibility constraints are not considered. The signature matching algorithm (without feasibility constraints) is applied to all vehicle types and achieves a re-identification accuracy of 67.3% (Figure 19a). When only atypical vehicles are considered, the re-identification accuracy reaches 97.4% (Figure 19c). In both cases, travel time can be easily derived from the mode of the travel time histogram. When, feasibility constraints were applied, the re-identification accuracy reaches 90.1% when all signatures are considered, and 99.6% for atypical vehicles. Of course, the selection of the feasibility window is intrinsically dependent upon the distance between the stations.

The second experiment was performed under the challenging scenario of queued and decelerating traffic. In the absence of feasibility constraints the re-identification was 14.3% (Figure 20a), while the performance was 36.1% (Figure 20b) when feasibility constraints were applied. Although these percentages are small, the modal value identifies the travel time in both cases (Figure 20a, Figure 20b).

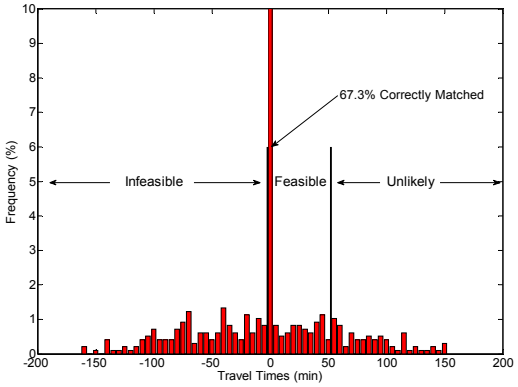

a) Histogram of travel times for all vehicles (N =976)

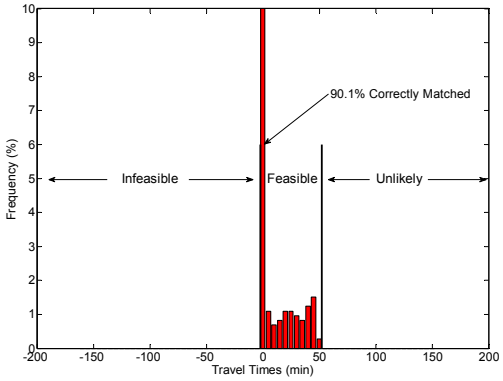

b)Filtered histogram of travel times for all vehicles (N = 657)

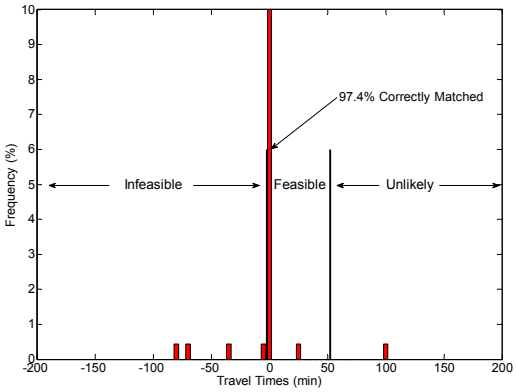

c) Histogram of travel times for all atypical vehicles (N =231)

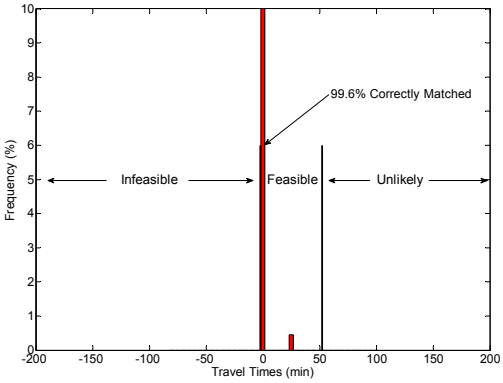

d) Filtered histogram of travel times for atypical vehicles (N = 225)

Figure 19: Filtering of the histogram of re-identified vehicles' travel times (MM128 Site).

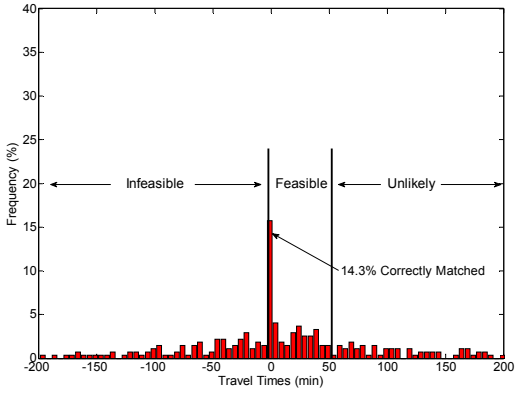

a) Histogram of travel times for all vehicles (N =273)

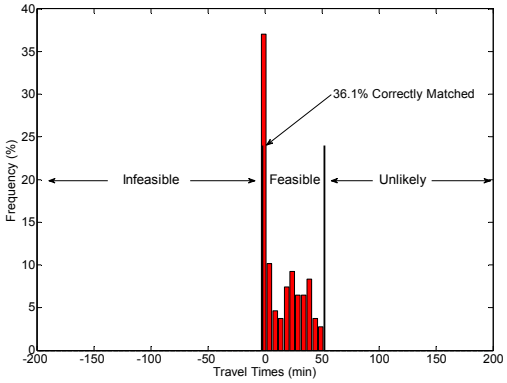

b)Filtered histogram of travel times for all vehicles (N = 108)

Figure 20: Filtering of the histogram of re-identified vehicles' travel times between NBM7/NBM5 and NBM2/NBM1 (West Lafayette Site).

6. Conclusions

6.1. Task A: Design Considerations for Detection of Bicycles Using Inductive Loops

From the experiments, it can be concluded that there is practically no difference between circular and octagonal loops for the bicycle detection problem. This results also show the effect of connecting the loops in series in comparison to connecting them independently. Loops connected independently provide larger detection zones than those connected in series. The independent connection provides increased sensitivity when the loops are placed deep beneath the pavement. Current practices place the loop as deep as 30 cm below the pavement to reduce maintenance costs. When bicycle detection is important, engineers should carefully consider how the detectors will be wired when this installation technique is used and at least consider wiring the loop closest to the stop bar to its own detector to improve the performance of bicycle detection.

6.2. Task B: Travel Time Estimation by Signature-Based Vehicle Re-identification

In this work, it was demonstrated that through proper pre-processing and signature matching, a computationally efficient and robust method to compute travel time from vehicle signatures is feasible and gives very good performance for free flowing traffic. Although the performance results were obtained from closely spaced detectors, they can be transferred to the realistic scenario since none of the assumptions in the procedure are dependent upon the length of the speed trap when no feasibility constrained are applied. Experiments with long detection zone spacing (1-4 miles) are on going and performance results will be reported in the future for further validation of this method. Performance

results for non-free flowing traffic conditions call for the design of a different and more sophisticated signature normalization algorithm for queued and decelerating traffic, where vehicles acceleration over the sensor at a single station is not constant. From Figure 19 and Figure 20, it can be observed that the travel time can be accurately determined from the histogram whenever the modal travel time frequency is much larger than pair bins.

7. Recommendations and Implementation Suggestions

7.1. Task A: Design Considerations for Detection of Bicycles Using Inductive Loops

The most important observation made from the work of Task A is that the detection performance of pave-over loop installations may be seriously compromised for bicycles when the loops are wired in series as is typical. For such installations where bicycle detection is also a consideration the loop closest to the stop bar should be wired individually to its own detector. In addition to this it is recommended that INDOT consider pavement markings to indicate where the bicycle detection zone exists on the pavement (even in the case of pavement-cut installation). Lastly, we recommend further study of the loop detection problem to quantify the tradeoff between increasing sensitivity for improving bicycle detection and the resulting increase in false positives due to automobiles in adjacent lanes.

7.2. Task B: Travel Time Estimation by Signature-Based Vehicle Re-identification

The results of Task B illustrate the feasibility of accurate travel time estimation by re-identification of micro-loop signatures. Given the large installed base of paired (speed-trap) inductive loop and micro-loop detection, the availability of commercial signature capture equipment, and the bandwidth needed to bring signatures to a centralized database for processing, further study of this travel time estimation technique is recommended. Future tests should implement the algorithms developed here on widely spaced detection stations (spacing on the order of 0.5 to 1 mile).

8. References

[Balke 1995] K. Balke, G. Ullman, W. McCasland, C. Mountain, and C. Dudek, "Benefits of Real-Time Travel Information in Houston, Texas," Southwest Region University Transportation Center, Texas Transportation Institute, College Station, TX, 1995.

[Coifman 1998] B. Coifman, "Vehicle Reidentification and Travel Time Measurement in Real-Time on Freeways Using the Existing Loop Detector Infrastructure," presented at 77th Annual Meeting of the Transportation Research Board, Jan. 11-15, 1998, Washington, D.C.

[Christiansen 1996] Christiansen and L. Hauer, "Probing for Travel Time: Norway Applies AVI and WIM Technologies for Section Probe Data", Traffic Technology International, Aug/Sep 1996, UK & International Press, Surrey, UK, 1996, pp. 41-44.

[Cui 1997] Y. Cui and Q. Huang, "Character Extraction of License Plates from Video" Proc. 1997 IEEE Computer Society Conference on Computer Vision and Pattern Recognition, IEEE, 1997, pp. 502-507.

[Dailey 1993] D. J. Dailey, "Travel-Time Estimation Using Cross-Correlation Techniques," in Transportation Research Part B, Vol. 27B, No. 2, 1993, pp. 97-107.

[El-Geneidy 2004] A. M. El-Geneidy, R. L. Bertini, "Towards validation of Freeway Loop Detector Speed Measurements using Transit Probe Data," *Intelligent Transportation Systems*, pp. 779-784, Oct 2004.

[Gajda 2001] J. Gajda, R. Sroka, M. Stencel, A. Wajda, T. Zeglen, "A Vehicle Classification based on Inductive Loop Detectors," *Instrumentation and Measurement Technology Conference,* vol. 1, pp. 460-464, May 2001.

[HCM 2000] Highway Capacity Manual, Transportation Research Board, National Research Council, Washington, DC, 2000.

[Jeng 2006] Jeng, S. T, and S. G. Ritchie, "A New Inductive Signature Data Compression method for on-line Vehicle Re-identification." In Proceedings of the 84th Annual Meeting of the Transportation Research Board, January22-26 2006, Washington, DC.

[Kan 1996] W. Y. Kan, J. V. Krogmeier, and P. C. Doerschuk, "Model-Based Motion Estimation from Image Sequences with an Application to Road Surveillance," Optical Engineering, Vol. 35, No. 6, pages 1723-1729, June 1996.

[Klein 1997] L. Klein, M. Kelley, and M. Mills, "Evaluation of overhead and in-ground vehicle detector technologies for traffic flow measurement," J. Test. Eval., vol. 25, no. 2, pp. 215–224, 1997.

[Klein 2005] L. Klein, D. Gibson, and P. Mills, "Traffic Detector Handbook," Federal Highway Administration, FHWA-HRT-04-130, 2005.

[Kreeger 1996] K. Kreeger and R. McConnell, "Structural range image target matching for automated link travel time computation," presented at the 3rd Annual World Congress on Intelligent Transportation Systems, Orlando, FL, Oct. 1996.

[Levine 1994] S. Levine and W. McCasland, “Monitoring Freeway Traffic Conditions with Automatic Vehicle Identification Systems”, ITE Journal, Vol. 64, No. 3, March 1994, pp. 23-28.

[Lin 2004] W. H. Lin, J. Dahgren, H. Huo, “Enhancement of Vehicle Speed Estimation with Single Loop Detectors,” *Data and Information Technology Transportation Research Record,* vol. 1870, pp. 147-152, 2004.

[Messer 1973] Messer, C., Dudek C., “Method for Predicting Travel Time and Other Operational Measures in Real-Time During Freeway Incident Conditions”, Highway Research Record 461, Highway Research Board, 1973, pp 1-16.

[Mills 1989] M. K. Mills, “Inductive Loop System Equivalent Circuit Model,” *Vehicular Technology Conference*, vol. 2, pp. 689-700, May 1989.

[NEC] Numerical Electromagnetics Code home page, http://www.nec2.org/

[Oh 2002a] C. Oh and S. G. Ritchie, "Real-Time inductive-signature-based level of service for signalized intersections", in Transportation Research Record 1802, Washington, D.C., TRB, National Research Council, June 2002, pp. 97-104.

[Oh 2002b] S. Oh and S. G. Ritchie,and C. Oh, " Real-time traffic measurement from single loop inductive signatures," in Transportation Research Record 1804, Washington, D.C., TRB, National Research Council, 2002, pp. 98-106.

[Oh 2004] C. Oh, S. G. Ritchie, and S.-T. Jeng, “Vehicle Reidentification using Heterogeneous Detection Systems,” presented 83rd Annual Meeting of the Transportation Research Board, Jan. 11-15, 2004, Washington, D.C.

[Park 2007] S. Park and S. G. Ritchie, “An Innovative Single Loop Speed Estimation Model with Advanced Loop Data. In Proceedings of the 85th Annual Meeting of the Transportation Research Board, January 21-25 2007, Washington, DC.

[Reno 2004] “Operating instructions for Model C-1000 series Two Channel Loop Detector,” Reno A&E, Feb 2004.

[Smith 2003] B. L. Smith, H. Zhang, M. Fontaine, and M. Green, “Cell Phone Probes as an ATMS Tool,” Research Report No. UVACTS-15-5-79, Center for Transportation Studies at the University of Virginia, Charlottesville, VA, 2003.

[Sun 1999] C. Sun, S. G. Ritchie, K. Tsai, and R. Jayakrishnan, “Use of vehicle signature analysis and lexicographic optimization for vehicle reidentification on freeways,” in Transportation Research Part C, Vol. 7, 1999, pp. 167-185.

[Turner 1995] S. M. Turner and D. J. Holdener, "Probe Vehicle Sample Sizes for Real-Time Information: The Houston Experience," Proc. Sixth IEEE International Conference on Vehicle Navigation and Information Systems, Seattle, WA, 1995, pp. 3-10.

[Tanaka 1994] Tanaka, Y., Nishimura, F. "Multiroute Travel-Time Data Provision Systems Operating in Osaka", Proc. 1994 IEEE Vehicle Navigation and Information Systems, 1994, pp. 351-356.

[Urbanek 1978] Urbanek, G., Rogers, R. Alternative Surveillance Concepts and Methods for Freeway Incident Management, Volume 1: Executive Summary, Federal Highway Administration, 1978.

[Wachtel 2000] Alan Wachtel, "Re-Evaluating Traffic Signal Detector Loops,'' *Bicycle Forum 50,* May 2000.